

PAPER • OPEN ACCESS

Influence of alloy chemistry on the deformation behaviour and anisotropic properties of aluminium ultra-fine-grained thin sheets

To cite this article: A Dhal *et al* 2018 *J. Phys.: Conf. Ser.* **1063** 012067

View the [article online](#) for updates and enhancements.

Related content

- [Anisotropic Properties of Superconducting \(La_{1-x}Sr_x\)₂CuO₄ Single-Crystal Thin Films](#)
Minoru Suzuki, Youichi Enomoto, Kazuyuki Moriwaki *et al.*
- [Evaluation of Mechanical Properties of MWCNT / Nanoclay Reinforced Aluminium alloy Metal Matrix Composite](#)
P S Samuel Ratna Kumar, D S Robinson Smart and S John Alexis
- [Microstructure and mechanical properties of accumulative roll bonded aluminium alloy AA5754](#)
T Hausöl, H W Höppel and M Göken



IOP | ebooks™

Bringing together innovative digital publishing with leading authors from the global scientific community.

Start exploring the collection—download the first chapter of every title for free.

Influence of alloy chemistry on the deformation behaviour and anisotropic properties of aluminium ultra-fine-grained thin sheets

A Dhal¹, S K Panigrahi^{1*} and M S Shunmugam¹

¹Department of Mechanical Engineering, Indian Institute of Technology Madras, Chennai 600036, India

*Correspondence Email: skapnigrahi@iitm.ac.in

Abstract. In the present work, cryorolling was performed on both pure Al (AA1070) and Al-Mg alloy (AA5083). Cryorolled materials were subjected to same level thermal treatment. The deformation behaviour and anisotropic properties of these materials were extracted from uniaxial tensile test results. These properties were compared for base, cryorolled and heat treated conditions for both the materials. Compared to AA1070, AA5083 shows much improved strain hardening capability. This is attributed to its lower stacking fault energy and influence of incoherent Mg solute in the Al matrix. By controlled thermal treatment substantial ductility was also regained for AA5083, without much loss in its tensile strength. This behaviour is attributed to the presence of bimodal microstructure in AA5083, consisting of ultra-fine as well as coarse grains. Due to the preservation of rolling texture even at high annealing temperature, the anisotropic properties were also found to be much favourable in case of AA5083.

1. Introduction

With the advent of global warming due to increased CO₂ footprint and alarming scarcity of fossil fuels, there is need to cut down the rate of fuel consumption in transportation sector. Development of materials with high specific strength is a key step in improving fuel efficiency. In automobiles and aircraft, sheet metals are major weight contributors as they are popularly used in form of panels and structural frames. Therefore, researchers are constantly pondering over methods to develop high strength sheet with good amount of ductility and formability [1]. Cryorolling followed by careful thermal treatment is an effective method to develop high strength ultra-fine-grained (UFG) sheet in large quantity. Cryorolling is an important severe plastic deformation (SPD) process due to its many advantages. First, production yield of cryorolling is much higher compared to other SPD processes. Second, there is no need of expensive tools and specialised equipment for this process. Third, cryorolling can be upscaled to a continuous mass production level. Most importantly, enhancement in mechanical strength of the final product is significantly higher than other SPD processes [2].

The extraordinary increase in strength during cryorolling is contributed by two factors: (i) refined grain size (Hall-Petch strengthening), (ii) accumulation of excessive dislocation in form of tangles and forests [3]. Due to the subzero deformation temperature, dynamic recovery is suppressed, resulting in very high dislocation density in the material after cryorolling. Grain refinement eventually occurs due to stress assisted dislocation rearrangement into nanoscaled subcells. The effectiveness of recovery suppression largely depends on the material's stacking fault energy (SFE). Materials with high SFE recovers easily, resulting in lower dislocation density after cryorolling. The degree of grained refinement in materials with high SFE is also lower. Therefore, such materials are expected to undergo



less strengthening after cryorolling. It is a known fact that presence of alloying elements in the material decreases its SFE. Therefore, alloying has profound effect on the post-cryorolling microstructure of a material. A deeper insight into the influence of alloy chemistry on the microstructural evolution after cryorolling has been provided in the authors' previous paper [4].

Although, the cryorolling imparts extraordinary high strength in the material, it comes at the cost of its ductility. Therefore, the formability of cryorolled material is expected to be very low. To increase the material's ductility some degree of thermal treatment is necessary after cryorolling. Post-cryorolling heat treatment leads to thermally assisted recovery and recrystallisation and finally grain growth. The recovery kinetics of cryorolled materials are relatively faster, leading to premature grain growth. However, in case of alloys, presence of solutes in the solvent matrix or precipitates at the grain boundaries helps in retarding the rate of grain growth and, thereby, improving the thermal stability of the UFG microstructure. With careful heat treatment of the cryorolled sheets it is possible to retain equiaxed, dislocation free, UFG microstructure or even develop a bimodal or duplex microstructure. Materials with such microstructure are known to have a combination of good strength and ductility [5].

Many researchers have investigated the mechanical properties and formability of a wide plethora of cryorolled materials, both before and after various types of thermal treatment [6-8]. However, to the best of authors' knowledge, none of the researchers have compared the mechanical (strength, ductility) and anisotropic properties (\bar{R} , ΔR) of pure metals and alloys subjected to similar level of cryorolling and post-cryorolling heat treatment. Such investigation is necessary to establish the influence of alloy chemistry on the mechanical and anisotropic properties of materials. This knowledge base will also be helpful in selecting the suitable material and optimising the post-cryorolling thermal treatment. One such attempt has been made in the present work, where pure Al metal (AA1070) and Al-Mg alloy (AA5083) were subjected to similar level of cryorolling and heat treatment. The properties of the materials were compared before and after cryorolling as well as after post-cryorolling heat treatments. The variation was carefully correlated with the microstructures at each condition.

2. Experimental details

Both the materials (AA1070 and AA5083) were procured in form of 10 mm plates. They were cut down into small square samples with edges of 500 mm. These square samples were kept in an enclosed furnace at a temperature of 500°C for 12 hours. This almost leads to complete dissolution of any second phase particle into the Al matrix and coarsen up the grains to make them sufficiently soft for effective cryorolling. These materials serve as the base condition for the present investigation. The base materials were then cryorolled using a 2-high rolling mill with a roll diameter of 110 mm operating at 8 rpm. The required reduction was obtained incrementally by rolling the material for several passes to reach a final thickness of 0.5 mm. The samples were dipped in liquid nitrogen bath for 10 minutes before every pass to ensure the sub-zero deformation temperature. Cryorolled samples were later subjected to annealing at temperatures of 200°C and 250°C for 30 minutes followed by their immediate quenching in cold water.

Dog-bone shaped (as per ASTM E8 standard) tensile specimens were cut from the processed sheets along 0°, 90° and 45° to the rolling direction. Tensile stress-strain curves were obtained by deforming all the various samples till fracture in an uniaxial tensile testing machine (Instron 5948) operating at a cross head velocity of 0.3 mm/min. To obtain the anisotropic properties, the specimens marked along the gauge length were subjected to partial deformation (within the uniform ductility range of all the materials). The true strains along the length and width of the samples were measured using a high-resolution microscope equipped with image processing software.

3. Results and discussions

3.1 Tensile properties of AA1070 and AA5083

Figure 1 shows the true tensile stress-strain curves obtained for specimens cut along the rolling direction. Clearly, the stress-strain curves of AA1070 (pure Al) is significantly different from that of AA5083 (Al-Mg alloy).

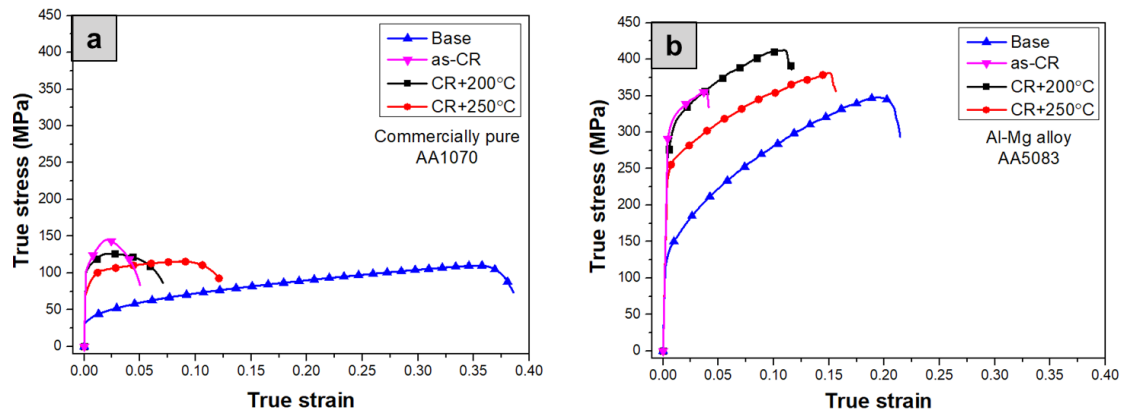


Figure 1: True stress-strain curves of AA1070 and AA5083 at various material conditions

Essential tensile properties such as yield strength (YS), ultimate tensile strength (UTS), uniform ductility (UD) and total ductility (TD) have been calculated from the stress-strain curves and have been illustrated in form of bar charts in figure 2. After cryorolling, the YS increase in both AA1070 and AA5083. The increment in YS for AA1070 after cryorolling is 70 MPa and for AA5083 is 173 MPa. Increase in YS after cryorolling depends on the balance between the dislocation accumulated during cryorolling and the dislocation annihilated due to dynamic recovery. Dynamic recovery is more prominent in AA1070 due to its greater SFE (166 mJ/m^2) compared to AA5083 ($\text{SFE} = 33 \text{ mJ/m}^2$). Therefore, although both the materials undergo same level cryo-deformation, due to greater magnitude of dynamic recovery in AA1070, the increase in YS is much lower in AA1070 compared to AA5083.

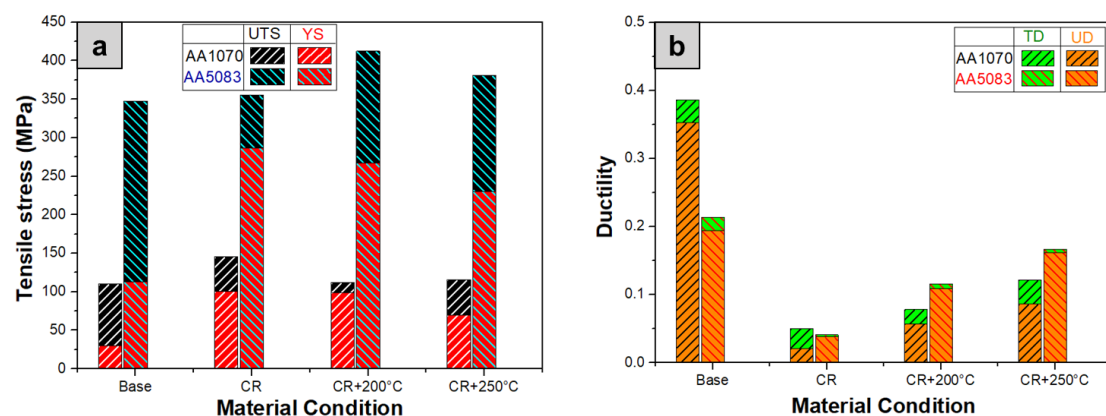


Figure 2: (a) Variation of yield and ultimate tensile stress, (b) variation of uniform and total ductility at various material conditions for both AA1070 and AA5083

After annealing at 200°C , there is a mere drop of 1-2% in the YS for both the materials. Due to high degree of stored energy in cryorolled samples, the recovery kinetics after annealing is expected to be very fast. On contrary, the YS remains primarily unchanged after annealing. The microstructural investigation presented in authors' previous paper reveals two important factors: (i) annealing at 200°C leads to annihilation of intertwined dislocations (tangles/forests) both in grain interiors and boundaries, resulting in development of nanometric grains with well-defined boundaries (ii) the influence of annealing on the grain size and morphology remains minimal. This implies that the YS of

the material is mainly influenced by the Hall-Petch strengthening factor, which is a function of the grain size, not the dislocation density. After heat treatment at 250°C, there is a steady drop in the YS of both AA1070 (29%) and AA5083 (14%). Annealing treatment at 250°C causes significant change in the grain size of the UFG microstructure. In AA1070, the grain growth is driven by grain boundary rotation and coalescence. In case of AA5083, solute influence abnormal grain growth is the governing mechanism of grain growth. Abnormal grain growth in AA5083 leads to development of a bimodal microstructure.

At base condition, the ductility is very high due to presence of very coarse, dislocation-free grains. Nevertheless, the ductility in AA5083 is relatively lower due to obstruction from Mg (solute) in the Al matrix. Cryorolling leads to significant loss in ductility of both the materials. Annealing of the cryorolled samples results in restoration of ductility. However, improvement of UD is much better in AA5083 compared to AA1070. After annealing at 250°C, UD of AA1070 is still less than 33% of its value in base condition. On the other hand, for AA5083, the UD after annealing at this temperature is 16% which is almost close to 85% at base condition. The combination of very good ductility bundled with high tensile strength of AA5083 could be attributed to its bimodal microstructure where high strength is contributed by the nanometric grains and good ductility is provide by the coarse grains.

3.2 Strain hardening abilities of AA1070 and AA5083

The tensile curves (Figure 1) reveals that the AA1070 shows much inferior strain hardening characteristics compared to AA5083. Modified Crussard–Jaoul (C-J) analysis was used to quantify the magnitude of strain hardenability [9]. This relationship is based on Swift's stress-strain relationship as represented in the following equation:

$$\varepsilon = \varepsilon_o + C\sigma_t^m \quad (1)$$

where σ_t is the true stress, ε is the true strain, ε_o is the initial true strain, m is the strain hardening exponent and C is the material constant. Equation for modified C-J relationship is obtained by differentiating equation 1 and applying logarithm on both sides.

$$\ln\left(\frac{\partial\sigma}{\partial\varepsilon}\right) = (1-m)\ln\sigma - \ln(Cm) \quad (2)$$

The strain hardening exponent (m) is an indicator of the magnitude of strain hardening and can be determined by taking the slope of log-log plot between $\left(\frac{\partial\sigma}{\partial\varepsilon}\right)$ and σ . The values of m have been plotted for various material conditions in figure 3.

It is very clear from the figure 3 that the strain hardening exponent of AA5083 is consistently higher compared to AA1070 at all four conditions. The strain hardening capacity of a material depends on its ability to accumulate mobile dislocation uniformly throughout the material. Strain hardening capacity is lost as soon as dislocations get accumulated preferably in a localised manner.

Strain localisation is primarily caused due to obstruction from artefacts (grain boundaries, particles, defects) or pre-existing dislocation tangles. At base condition, AA1070 (pure Al) is free from such excessive dislocations in form of tangles and the only source of dislocation accumulation are the grain boundaries. Due to the grains being very coarse, the volume fraction of grain boundary is very less. Therefore, the strain hardening potential of both the materials is highest for the base, undeformed condition. However, strain hardenability is consistently greater for Al-Mg alloy (AA5083) compared to the pure Al (AA1070). It is because AA5083 is a solid solution, where apart from the grain boundaries the grain interiors also accumulate dislocations. The grain interiors contain Al matrix embedded with solute atoms (Mg). Mg (hcp crystal) is highly incoherent with Al (fcc crystal) matrix

due to their distinctively different crystallography. Therefore, it undergoes increased strain hardening promoted by solute strengthening effect.

After cryorolling, the strain hardening ability of both the material decreases significantly. This is due to the accumulation of excessive dislocations stored in forms of tangles and forests which leads to premature strain localisation. This effect is more profound in AA5083 since it accumulates much greater amount of dislocation due to its lower SFE. However, after annealing treatment, these excessive dislocations get annihilated and the strain hardening capability of the material improves. Bimodal microstructure of AA5083 has even greater strain hardening exponent compared to its base counterpart. This could be attributed to the presence of both UFG and coarse grains which facilitates free movement of a larger amount of mobile dislocations in the microstructure.

3.3 Mechanical and planar anisotropy of AA1070 and AA5083

Both mechanical anisotropy (\bar{R}) and planar anisotropy (ΔR) are crucial parameters which are used as benchmark to assess the formability of a sheet. The values of \bar{R} and ΔR depend on the material's microstructural features such as crystallographic texture, grain morphology and stored dislocation density [10]. \bar{R} represents the resistance to thinning of the sheet (equation 3) and ΔR signifies the resistance to earing during sheet forming (equation 4) and they are calculated from the average of the ratios between the true strain determined along length (l) and width (w) of tensile specimens oriented at various angles ($0^\circ, 45^\circ, 90^\circ$) to the rolling direction (equation 5).

$$\bar{R} = \frac{R_0 + 2R_{45} + R_{90}}{4} \tag{3}$$

$$\Delta R = \frac{R_0 - 2R_{45} + R_{90}}{2} \tag{4}$$

$$R_{0,45,90} = \left(\frac{\ln(w_o / w_f)}{\ln(l_f w_f / l_o w_o)} \right)_{0,45,90} \tag{5}$$

Based on the above equation, the values of \bar{R} and ΔR have been calculated at the base condition and post-cryorolling annealing conditions corresponding to both the materials (represented graphically in figure 4 and values provided in table 1). The analysis of cryorolled samples has been avoided due to its limited uniform ductility.

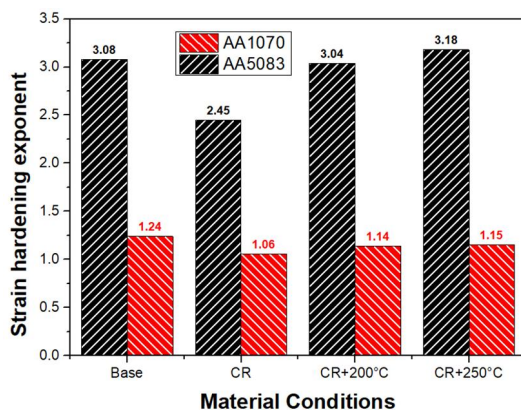


Figure 3: Strain hardening exponent determined by modified C-J analysis at various material conditions

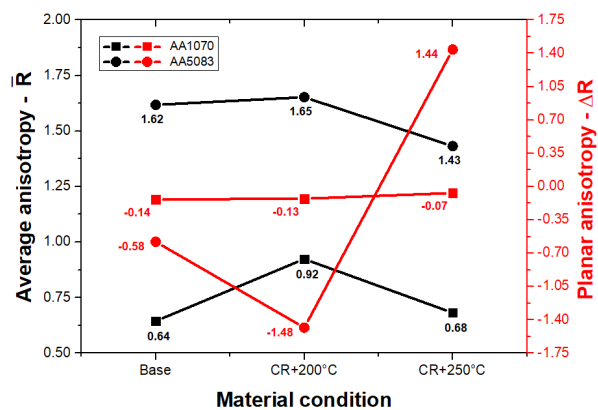


Figure 4: The values of average and planar anisotropy for AA1070 and AA5083 at various material condition

Table 1. Mechanical anisotropy (\bar{R}) and Planar anisotropy (ΔR) of both AA1070 and AA5083 alloy at various processing conditions

Material Condition	Mechanical anisotropy (\bar{R})		Planar anisotropy (ΔR)	
	AA1070	AA5083	AA1070	AA5083
Base	0.64	1.62	-0.14	-0.58
CR + 200°C	0.92	1.65	-0.13	-1.48
CR + 250°C	0.68	1.43	-0.07	1.44

The above figure shows that the value of \bar{R} of AA5083 is significantly higher than that of AA1070. This indicates that AA5083 can be easily deformed without thinning and possesses greater formability compared to AA1070. There is a moderate increase in the magnitude of \bar{R} after cryorolling, followed by annealing at 200°C. This could be attributed to the influence of the rolling texture which improves the resistance against localised deformation in the thickness direction. A decrease in the value of \bar{R} is observed after annealing at 250°C, which may be attributed to the partial loss of rolling texture and inception of more random texture in the material. On the other hand, the value of ΔR is found to be much closer to zero for AA1070 which indicates greater resistance to earing. In case of AA5083, ΔR is much greater than zero, which indicates the susceptibility of AA5083 sheets to earing.

4. Conclusions

AA5083 and AA1070 show significant variations in their tensile, strain hardening and anisotropic properties. Due to greater degree of dynamic recovery promoted by its higher SFE, the increase in yield strength of AA1070 after cryorolling is relatively lower compared to AA5083. However, after annealing at 250°C, it is possible to get very strong as well as ductile AA5083 sheets which can be attributed to its bimodal microstructure consisting of both UFG and coarse grains. The strain hardening potential of AA5083 is much superior than AA1070, which is attributed to the influence of incoherent Mg solute dissolved in Al matrix. Although cryorolling reduces the strain hardening potential due to presence of excessive dislocation in form of tangles, it is easily recovered after annealing treatment. The average anisotropy is more favourable in case of AA5083 compared to AA1070 in all material conditions, which signifies its enhanced sheet metal formability. Cryorolling followed by annealing at 200°C further enhances the formability due to the influence of rolling texture imparted during cryorolling. Based on the values of planar anisotropy, resistance to earing is expected to be inferior in AA5083 compared to AA1070.

References

- [1] Starke E A Jr, Staley J T 1996 *Prog. Aero. Sci.* **32** 131-172
- [2] Dhal A, Panigrahi S K, Shunmugam M S 2015 *Mat. Sci. Engg. A* **645** 382-392
- [3] Hansen N 2004 *Scr. Mater.* **51** 801-806
- [4] Dhal A, Panigrahi S K, Shunmugam M S 2017 *J. Alloys Comp.* **726** 1205-1219
- [5] Wang Y, Chen M, Zhou F, Ma E 2002 *Nature* **419** 912-915
- [6] Srinivas B, Dhal A, Panigrahi S K 2017 *Int. J. Plast.* **97** 159-177
- [7] Vigneshwaran S, Sivaprasad K, Narayanasamy R, Venkateswarlu K 2018 *Mat. Sci. Engg. A* **721** 14-21
- [8] Naga Krishna N, Ashfaq M, Susila P, Sivaprasad K, Venkateswarlu K 2018 *Mat. Char.* **107** 302-308
- [9] Jin J E, Lee Y K 2009 *Mat. Sci. Engg. A* **527** 157-161
- [10] Lenzen M and Merklein M 2017 *AIP Conf. Proc.* **1896** 16000

Acknowledgments

This work has been financially supported by Aeronautical Research and Development Board, India (ARDB/01/2031831/M/I). The mechanical testing facility has been funded by FIST grant, Department of Science and Technology, India (SR/FST/ET11-059/2012 (G)).